



# Voice-assisted translation of English vocabulary for offshore surface water temperature and trade

Chen Qin<sup>1</sup> · Jia Zhu<sup>2</sup>

Received: 23 April 2021 / Accepted: 26 June 2021 / Published online: 15 July 2021  
© Saudi Society for Geosciences 2021

## Abstract

Due to the gradual improvement of computing power and the development of big data, the error rate of voice recognition systems and voice assistance functions gradually decreases with the gradual application of deep learning. In terms of commercial contracts, it is a legally binding text. This article first analyzes the theory of functional equivalence translation and then analyzes the theory of functional equivalence translation from the perspective of professionalism and accuracy and determines the principles of business contract English vocabulary translation. At the same time, it studies English in terms of vocabulary equivalence. In the process of teaching trade English, some common vocabulary in trade English is easy to be misunderstood. This article analyzes these common translation errors and their main causes and proposes some appropriate solutions. Business English vocabulary translation must follow the principle of pragmatic equivalence, and the translation must be flexible to deal with communication obstacles caused by cultural background, language habits, and other factors, because they are subject to two different language and cultural characteristic rules (English and Chinese). The seasonal autoregressive summed moving average (ARIMA) model is used to simulate the time series of the surface water temperature in the coastal waters, and the structure of the model is determined through the principle of irrelevance and simplicity. On this basis, the optimal ARIMA prediction model is established and the surface water temperature of the coastal waters is monthly. The prediction results are consistent with the monthly change trend of the sea surface temperature, indicating that the model is suitable for predicting the offshore surface temperature.

**Keywords** Language assistance · Surface water temperature · Business English · Vocabulary translation

## Introduction

In recent years, end-to-end speech recognition technology has attracted widespread attention in the industry. The end-to-end modeling technology is a sequence modeling technology that makes full use of the neural network structure to directly map the special speech frames of the input language to the output text sequence, which belongs to the category of language

assistance. Due to the continuous improvement of speech recognition performance, each sentence of the transcribed text usually contains only a small number of incorrectly transcribed words. This means that using incorrect and correct assignments in the copied text to train the detection network will encounter the problem of extremely unbalanced classification data. For the equivalent translation theory, it was developed by the famous American structuralist language master and the world-renowned translator Nida (Al-Dossary and Marfurt 2006). Nida mainly works in the USA, and his main occupation in his life is to translate the “Bible.” In the course of this scholar’s work in Bible translation, he discovered many translation theories based on reality, and they have become a hot spot in the history of translation studies (Blakely 1995). When translating various aspects of the language, it does not specifically emphasize the exact correspondence between the text surface and the vocabulary translation and realizes a functional equivalence between the two languages, that is, dynamic pairing and “functional equivalence.” In fact, the most basic

Responsible Editor: Hoshang Kolivand

This article is part of the Topical Collection on *Smart agriculture and geo-informatics*

✉ Jia Zhu  
zhuja0419@126.com

<sup>1</sup> Chengdu Aeronautic Polytechnic, Chengdu 610042, China

<sup>2</sup> Civil Aviation Flight University of China, Guanghan 618307, Sichuan, China

theory of functional equivalence translation is that the meaning and formal equivalence of translation are required, and semantic equivalence is more important than formal equivalence (Blumentritt et al. 2006). As a practical style of stylistic expression, business English not only has a unique vocabulary, its syntactic function is more special than ordinary languages, but also has a unique professional knowledge and cultural background (Cevallos et al. 2013). At the same time, research on the prediction of offshore surface water temperature is essential for the organization and management of aquaculture, coastal tourism, and other activities (Cooper and Cowan 2009). Under the influence of many factors, tidal currents and the interaction between ocean and land, sea surface temperature (SST) changes have obvious random nature, and it is usually difficult to use structural causal models for effective simulation (Eales 2001). As a data-driven analysis technology, the influence of time series analysis has gradually deepened, because it avoids the mutual influence between many factors of sequence variables and greatly simplifies the sequence analysis and simulation process (Gonzalez and Woods 2008). The autoregressive summed moving average (ARIMA) model is a classic time series analysis model. Based on the inter-relationship between time series data, reveal the potential changes of the sequence through mathematical statistical analysis, and realize the simulation and prediction of the sequence based on the analysis (Lee et al. 2013).

## Materials and methods

### Data source

This study uses the results of five representative models selected in CMIP5 under the RCP4.5 scenario to investigate changes in the vicinity of sea temperature in eastern China (Li 2015). Choose 2010 as the current climate conditions, and choose 2030, 2060, and 2090 as future climate conditions (Miller and Singh 1994). Use the 2006–2015 average to replace the 2010 simulation results to reduce the simulation bias of each model (Mironova and Jaroslav 1993). Similarly, use the average values of 2026–2035, 2056–2065, and 2086–2095, respectively, instead of the simulation results for 2030, 2060, and 2090. RCP4.5 is compared with the

simulation results produced in RCP2.6 (low) and RCP8.5 (high) (Phillips et al. 2007). Refer to the simulation results according to the rate. The RCP4.5 simulation result is more moderate and closer to the current situation. See Table 1 for more information about these modes.

See Table 2 for the range of latitude and longitude of different sea areas.

### Quality control and data processing

Before the formal analysis of the CTD data used in research, there is a very important task, which is the preliminary quality inspection and management of the data. Observation data must be preprocessed according to analysis requirements. This step is an important basis for subsequent analysis and calculations and can directly affect the analysis results of the research (Roberts 2001). This article performs the following steps: data content and format integration, save the CTD file of each site in Excel spreadsheet format, and then extract the ocean elements required for the survey (Sandgren and Snowball 2001). Since CTD data is divided into ascending and descending data, this research is based on the ascending and a comparative comparison of the quality of data in a descending order, prioritizing the data in the ascending order (Field and Roggenthen 1986). If the quality error of the rising data is too large or insufficient, use the falling data to supplement (Seisuma and Kulikova 2012).

For data quality control, clear data that obviously has abnormal temperature and salt value, such as directly deleting salt or  $-1$  temperature value. Temperature and salinity are very important data elements in hydrological analysis, and their quality is directly related to the final research results (Sergeev 2015). According to previous studies, the salinity range of 40 to 60°S in the Antarctic ocean is between 33 and 35, so salinity values below 33 or above 35 are excluded (Sergeev et al. 2017).

After preliminary screening of the data, the temperature-salt distribution map can be easily drawn, and more obvious outliers can be checked and deleted. Since outliers may be caused by anomalies in the marine environment, points that cannot be evaluated as outliers can be retained (Šliaupa and Hoth 2011). If there is a change, wait for a formal data analysis before making a decision.

**Table 1** CMIP5 data model information

Model	Area	Average resolution
ACCESS1.3 (Australian National University)	77.9°N–65.2°S, 0.5°E–359.5°E	0.3° (lat) × 1.0° (lon)
BCC-CSM1.1 (China National Climate Center)	81.5°N–89.5°S, 295.5°W–79.5°E	1.0° (lat) × 1.0° (lon)
CCSM4 (National Center for Atmospheric Research)	79.2°N–89.7°S, 1.1°E–359.9°E	0.5° (lat) × 0.9° (lon)
GFDL-ESM2G (Princeton University, USA)	76.8°N–89.8°S, 279.5°W–79.5°E	0.5° (lat) × 1.0° (lon)
MPI-ESM-MR (Max Planck Institute, Germany)	78.7°N–89.8°S, 0.0°E–360.0°E	0.1° (lat) × 0.1° (lon)

**Table 2** The latitude and longitude range of each sea area

Sea area	Latitude	Longitude
Bohai	37–41°N	117–122°E
Yellow Sea	32–39°N	119–126°E
East China Sea	23–33°N	118–130°E

**Speech recognition model design**

As shown in Fig. 1, to build a traditional speech recognition system, you must first model the phonemes and manually configure the pronunciation dictionary (Stauskaitė 1962). Next, the speech is preprocessed, and then speech feature extraction is performed. After training the mixed sound HMM-DNN model, a decoding operation is needed to combine the output of the frame-level neural network into the text sequence.

**Speech feature extraction**

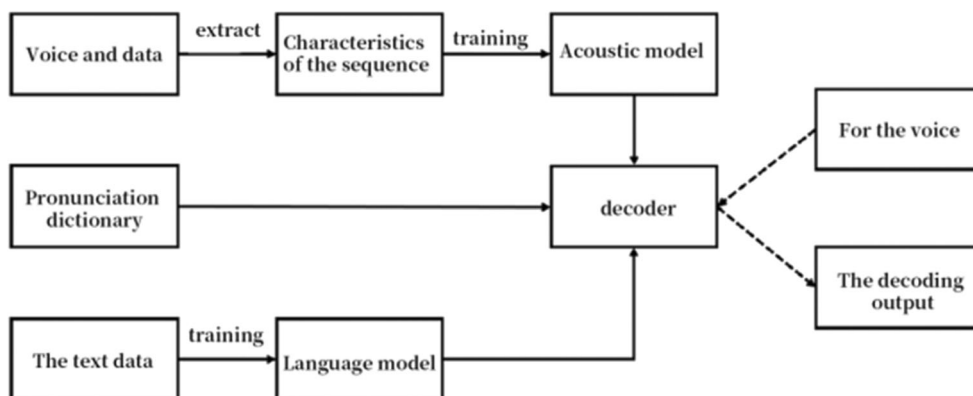
For input audio, high-frequency formants should be highlighted to balance the spectrum. The audio signal passes through a high-pass filter to pre-emphasize the audio. The calculation process is as follows:

$$y(t) = x(t) - \alpha x(t-1) \tag{1}$$

$$H_m(k) = \begin{cases} 0 & k < f(m-1) \\ \frac{2(k-f(m-1))}{(f(m+1)-f(m-1))(f(m)-f(m-1))} & f(m-1) \leq k \leq f(m) \\ \frac{2(f(m+1)-k)}{(f(m+1)-f(m-1))(f(m)-f(m-1))} & f(m) \leq k \leq f(m+1) \\ 0 & k \geq f(m+1) \end{cases}, \tag{4}$$

Among them,  $\sum_{m=1}^{M-1} H_m(k) = 1$ .

**Fig. 1** Basic flow chart of traditional speech recognition



The coefficient  $\alpha$  of the filter is usually set to 0.95 or 0.97. In view of the fact that the speech signal is a short-term stationary signal, the direct Fourier transform (fast Fourier transform (FFT)) of the non-stationary whole signal is easy to be interfered. Therefore, the obtained features are meaningless. Assuming that the Fourier transform data is infinite, in order to increase the continuity between the left edge and the right edge of the frame, another step of windowing is needed to the signal; the form is as follows:

$$y(t) = x(t) - \alpha x(t-1) \tag{2}$$

Among them,  $0 \leq n \leq N-1$ ,  $N$  is the set window length, and  $\alpha$  is the coefficient.

It is difficult to see the characteristic changes of a signal in the time domain. Therefore, the Fourier transform is usually used for the signal data to convert the time domain signal to the frequency domain to obtain the energy distribution of the signal. After preprocessing, discrete Fourier transform (DFT) is performed on each frame signal. The conversion formula is:

$$X_i(k) = \sum_{n=0}^{N-1} x_i(n) e^{-j2\pi kn/N}, 0 \leq k \leq N-1 \tag{3}$$

Using a triangular filter, the number of filters in the filter bank is defined as  $M$ , and the center frequency is  $(f(m)) = 1, 2, \dots$ . The interval between  $(f(m))$  increases as  $m$  increases. The frequency response of the triangular filter is defined as follows:

Then, calculate the logarithmic energy output of each filter bank as shown below.

$$s(m) = \ln \left( \sum_{k=0}^{N-1} |X_i(k)|^2 H_m(k) \right), 0 \leq m \leq M \quad (5)$$

Through the discrete cosine transform, the coefficients of the filter bank are decorrelated to form a compressed representation of the filter bank. The MFCC calculation formula is as follows:

$$C(n) = \sum_{m=0}^{N-1} s(m) \cos \left( \frac{\pi n(m-0.5)}{M} \right), n = 1, 2, \dots, L \quad (6)$$

L refers to the order of MFCC coefficients, and M is the number of triangular filters.

### Acoustic model design

The traditional acoustic model of speech recognition uses the GMM-HMM model. This type of recognizer uses a hidden Markov model to model the time series MFCC features and then uses a Gaussian mixture model to model the probability distribution of the voice feature vector corresponding to the detected hidden Markov state (Stauskaitė 1966).

For a continuous random variable  $x$ , if it conforms to the Gaussian mixture distribution, the corresponding probability density function  $p(x)$ :

$$p(x) = \sum_{m=1}^M \frac{c_m}{(2\pi)^{\frac{1}{2}} \sigma_m} \exp \left[ -\frac{1}{2} \left( \frac{x - \mu_m}{\sigma_m} \right)^2 \right]$$

$(\mu_m, \sigma_m)$  is a Gaussian distribution with mean  $\mu_m$  and variance  $\sigma_m^2$ .  $c_m$  is a positive real number, and  $\sum_{m=1}^M c_m = 1$ . Because in speech recognition, what needs to be calculated is the variable  $X$  composed of multiple continuous random states, so we use the multivariate Gaussian mixture distribution, and the probability density function of the  $X$  variable is as follows:

$$p(X) = \sum_{m=1}^M \frac{c_m}{(2\pi)^{\frac{D}{2}} \left| \sum_m \right|} \exp \left[ -\frac{1}{2} (X - \mu_m)^T \sum_m^{-1} (X - \mu_m) \right] \quad (8)$$

For the parameter  $\theta = \{X, \mu_m, \sum_m\}$  in the Gaussian mixture model, the parameters are estimated by the maximum expectation algorithm (EM). This article does not elaborate on the EM algorithm.

In order to describe the factor state transition relationship, the phoneme sequence can be annotated by the hidden Markov model and the Viterbi algorithm. Therefore, it is expressed in the form of multivariate mixture Gaussian distribution. For the state  $i$ , the emission probability of the observed acoustic feature vector  $O_t$  is expressed as the formula

$$p_i(O_t) = \sum_{m=1}^M \frac{c_{i,m}}{(2\pi)^{\frac{D}{2}} \left| \sum_{i,m} \right|^{\frac{1}{2}}} \exp \left[ -\frac{1}{2} (O_t - \mu_{i,m})^T \sum_{i,m}^{-1} (O_t - \mu_{i,m}) \right] \quad (9)$$

The parameters of the hidden Markov model can be estimated using the extended EM algorithm Baum-Welch.

## Results

### The temperature distribution characteristics of different depth layers of the ocean surface

Obviously, the temperature changes at the 20-m level in 2017 and 2018 are similar, while the difference between 2019 and 2020 is quite large. In 2019, since the summer has just entered, the surface water temperature is still relatively low, with a temperature range of  $0 \sim 1.25$  °C. 2020 is the midsummer of Antarctica. After a whole summer of solar radiation, sea surface water has a significantly higher temperature than other periods in the same depth layer, ranging from 1.75 to 2.75 °C. The temperature changes in 2017 and 2021 are similar, ranging from 0.5 to 2 °C. It can be found from Fig. 2 that the water temperature in the shelf area north of the SSI in 2019 is higher than that in other regions, but the water temperature in the shelf area north of the SSI in 2018, 2019, and 2020 is lower than that in other regions. The summer has just entered in 2019, and the sea surface water body still retains the characteristics of the previous winter to some extent (Tanner 1990). The WAP shelf system is not affected by the downward wind due to the topography, so the climatic conditions in the area are warm and suitable, which is also another degree. The above guarantees that the water temperature in this area is higher than that in the deep sea area (Vetrimurugan et al. 2017).

The temperature distribution at the depth of 60 m (Fig. 3) is more complicated, with cores of cold and warm water appearing at different locations. The formation of these cores of cold and warm water may be due to vortices, vertical mixing of seawater, or ocean fronts. Except for 2017, the other 3 years (2018, 2019, 2020) have continued the characteristics of the 20-m layer, the higher the latitude, the lower the temperature. In 2018, 2019, and 2020, different degrees of cold water core appeared. It is considered that the cold water mass WW under the AASW may be upwelled under the action of upflow. The temperature isotherm at this time extends in the northeast direction and is consistent with the movement direction of the ACC, that is, the water body in the 60-m layer is still affected by the ACC. The characteristics of the cold water core in 2018 are not obvious. It may be that the summer has

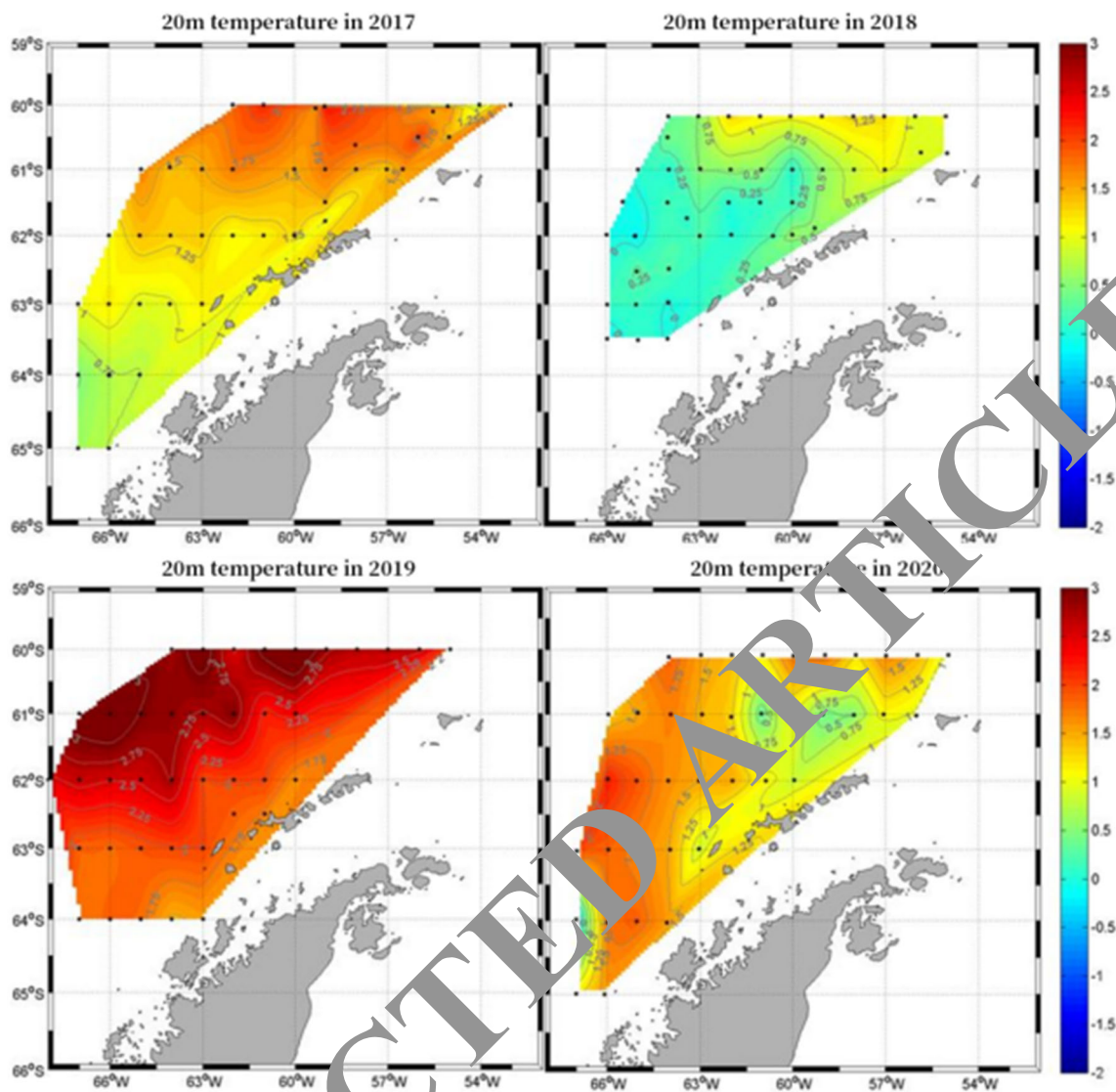


Fig. 2. Spatial distribution of temperature at 20 meters

just entered, and the vertical stratification of AASW and WW caused by sea ice melting and other reasons is not as obvious as in other years that fully entered the midsummer. In the 4 years, the water temperature of the shelf area was higher than that of other deep water areas. This may be related to the intrusion of CDW into the shelf area to provide heat supply for the water body of the shelf area.

Figure 4 shows that the seawater temperature of this layer is generally low. The 4-year average seawater temperature is about  $-0.25^{\circ}\text{C}$ . Judging from its temperature value, this layer should be a typical WW cover layer.

As shown in Fig. 5, the seawater temperature of this layer is much higher than that of the 100-m layer. The water temperature range of 2017, 2018, 2019, and 2020 is  $0 \sim 1.5^{\circ}\text{C}$ , and the water temperature in 2020 is higher than the other 3 years, which is  $0.75 \sim 2^{\circ}\text{C}$ ; it is obvious from the above that it is the CDW that affects the properties of the water layer. The water

temperature in the shelf area is lower than that in other areas. This is different from the phenomenon that the shelf area is higher than other areas observed in other depth layers (20 m, 60 m, 100 m). The impact of low-temperature water from Bransfield Strait was brought by the stream.

### The temperature structure of different sections of the ocean surface and its interannual variation

Section D1 crosses the STR. Above the STR (points D1-05 and D1-06), it can be seen that there is a downward depression in the thermo-salt contour. This phenomenon is obvious in 2019 and 2020, but this phenomenon was not observed in 2018 just after the summer, so it is speculated that the formation of the stationary vortex is related to the season, and the phenomenon is most obvious in the midsummer of Antarctica. The distribution of water masses on this section shows a

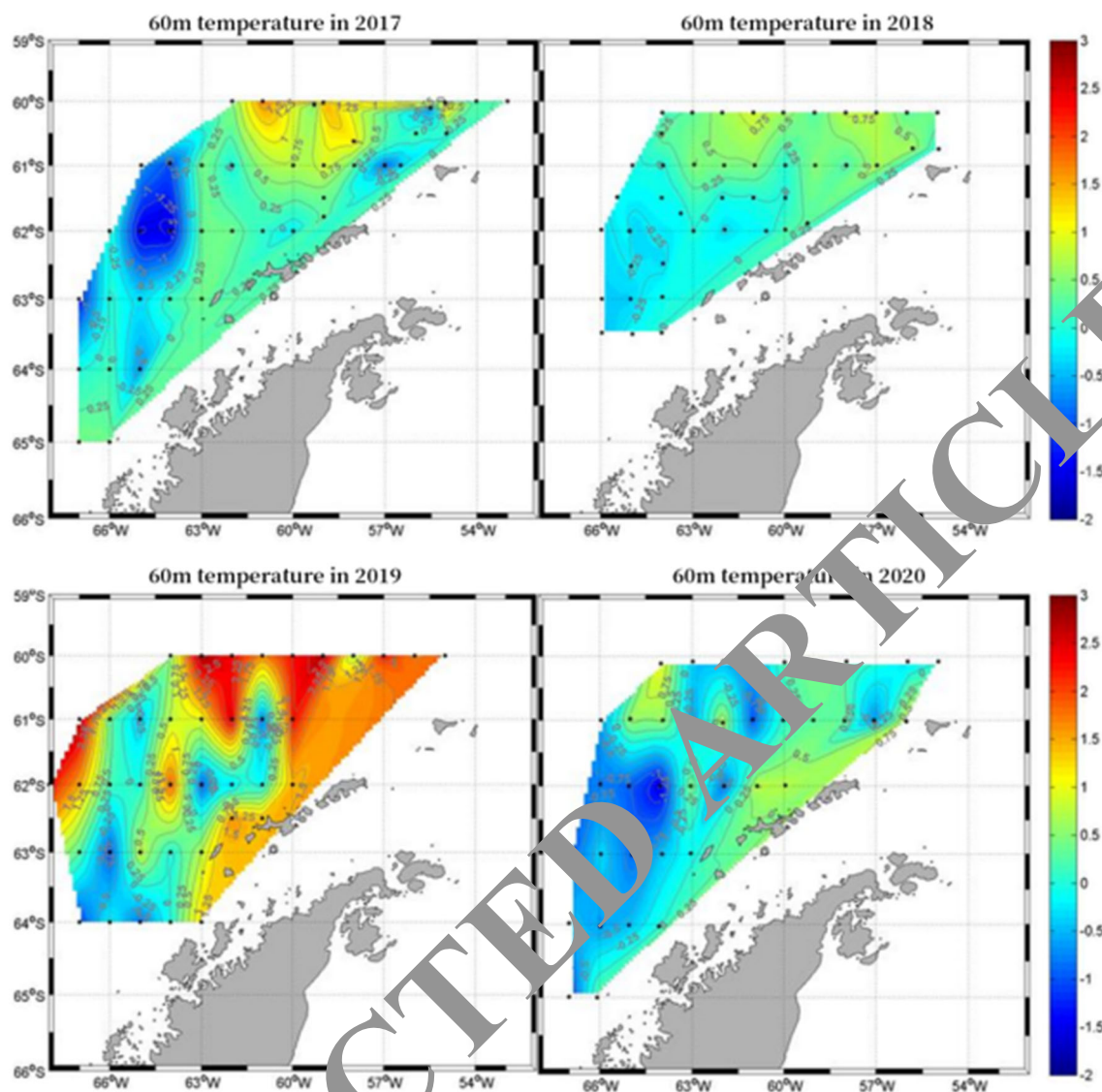


**Fig. 3** Spatial distribution of temperature at the 60-m layer

vertical distribution structure of Antarctic surface water (ASSW), winter water (WW) and circumpolar deep water (CDW) from top to bottom. From the salinity contour, the salinity distribution gradually increases from top to bottom. The salinity value of the water body on the east side of STR is obviously higher than that of the water body on the west side. The water body on the east side is affected by the low-temperature and high-salinity Weddell seawater, while the water body on the west side is affected by the low-salt Scott seawater, as shown in Fig. 6.

The temperature changes on the east and west sides of STR are not obvious, but there are differences between the years. ASSW observed the lowest temperature in 2018 (just entering summer). The salinity value of ASSW in that year was uniform at 33.9, but across the STR, as the salinity rises, a clear salinity gradient can be seen from the salinity contour. ASSW had the highest temperature in 2019 (end of

summer), with a maximum temperature of 3.25 °C. In that year, the ASSW temperature at the station on the west side of STR was higher than that at the station on the east side. In 2018, the thickness of ASSW was only about 40 m; in 2019, it received the longest sunlight in summer, and its thickness was about 60 m; in 2013, the thickness of ASSW was about 50 m. Because the winter water below ASSW is protected by a clamshell, the temperature change is not significantly affected by time, especially in the WW in the same season. Its water temperature maintains the basic characteristics of the water mass in the last winter. The water depth in the winter of 2017 is about 80–140 m, the water depth in winter of 2018 is about 70–130 m, and the depth of WW in 2017 is about 50–130 m. The CDW is located under the WW. In 2018, the depth of the CDW was less than 160 m, and in 2019, it was less than 130; the depth of the CDW in 2019 was about 150 or less, as shown in Fig. 7.

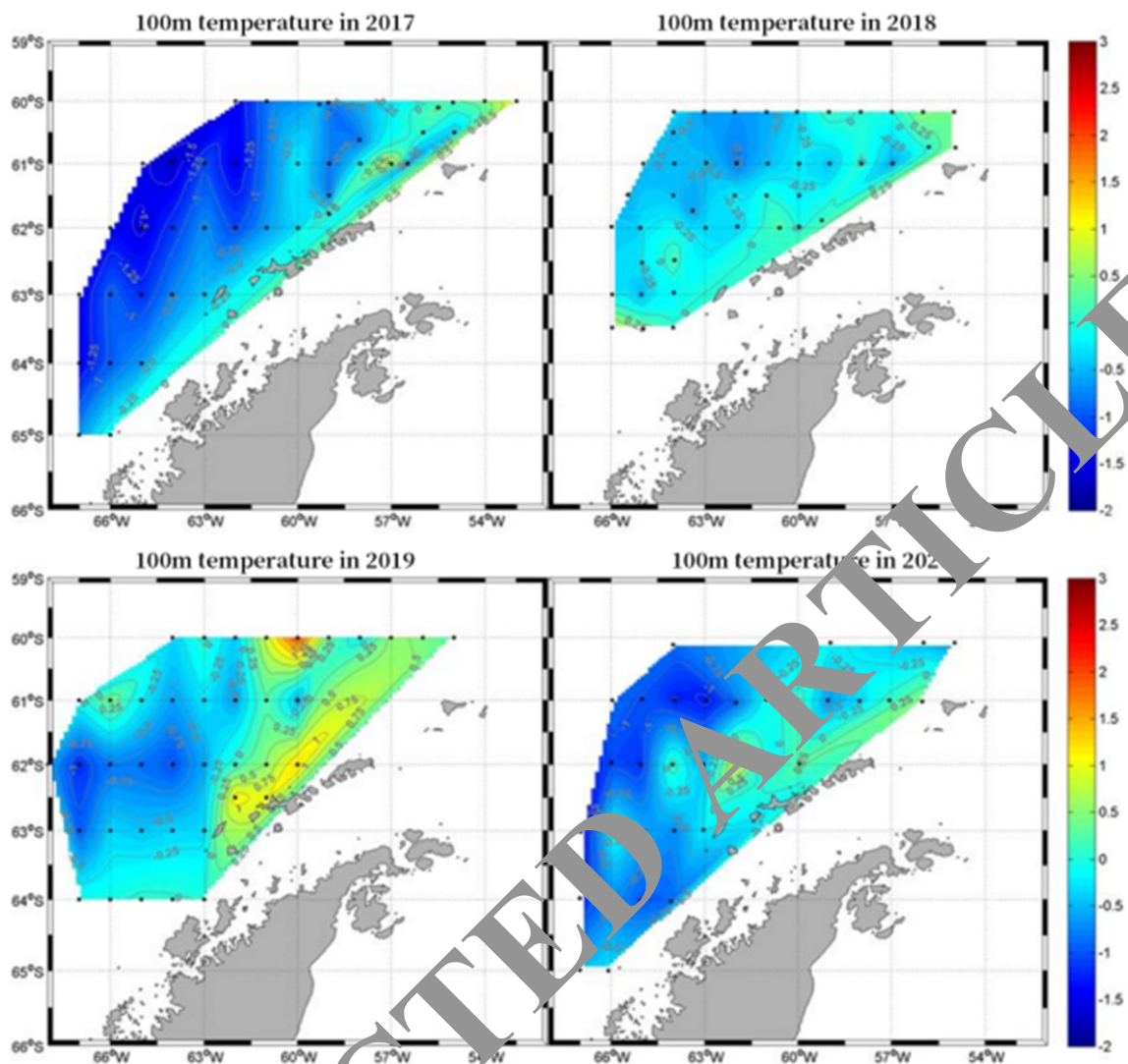


Fig. 4 Spatial distribution of temperature at 100 m layer

### Model verification of offshore surface water temperature

The model verification results are shown in Table 3. Through the model verification results, we found that the five models have certain errors relative to the measured data, but the error range is not large, and they can all be used for subsequent SST future prediction studies. Among them, the MPI-ESM of the Max Planck Institute in Germany-MR model prediction results is close to WOA13 V2 field observation results and has the highest resolution. In the following SST spatial distribution prediction analysis, we will use the MPI-ESM-MR model results to analyze the future spatial distribution of sea temperature in the continental shelf sea of eastern China.

From Table 4 and Fig. 1, we find that the Bohai Sea, the Yellow Sea, and the East China Sea will have obvious SST warming trends in the next 80 years: From 2010 to 2030, the average SST temperature rise of each sea area is 0.39–0.44°C,

of which the East China Sea has the largest temperature rise and the Bohai Sea has the smallest; in 2060, the average temperature rise of SST in all sea areas is 1.03–1.42°C, among which the Yellow Sea has the largest temperature rise and the East China Sea has the smallest temperature rise.

Table 4 and Fig. 8 show the annual average SST of each model in the coastal waters of eastern China (Bohai Sea, Yellow Sea, East China Sea) in 2010, 2030, 2060, and 2090 (the upper part of Table 4, Fig. 1a–c) and the value of the SST change and the inter-annual rate of change in 2090 relative to 2010 (the lower part of Table 4, Fig. 1d–f). Among them, the rate of change is divided by the amount of change in 2030–2010, 2060–2030, and 2090–2060 by the corresponding number of years. The amount of change is to reflect the inter-decadal change of SST in the future relative to the current year, and the rate of change is to better reflect the inter-annual change rate of SST. In Fig. 8, the red horizontal broken line represents the average of the five models.

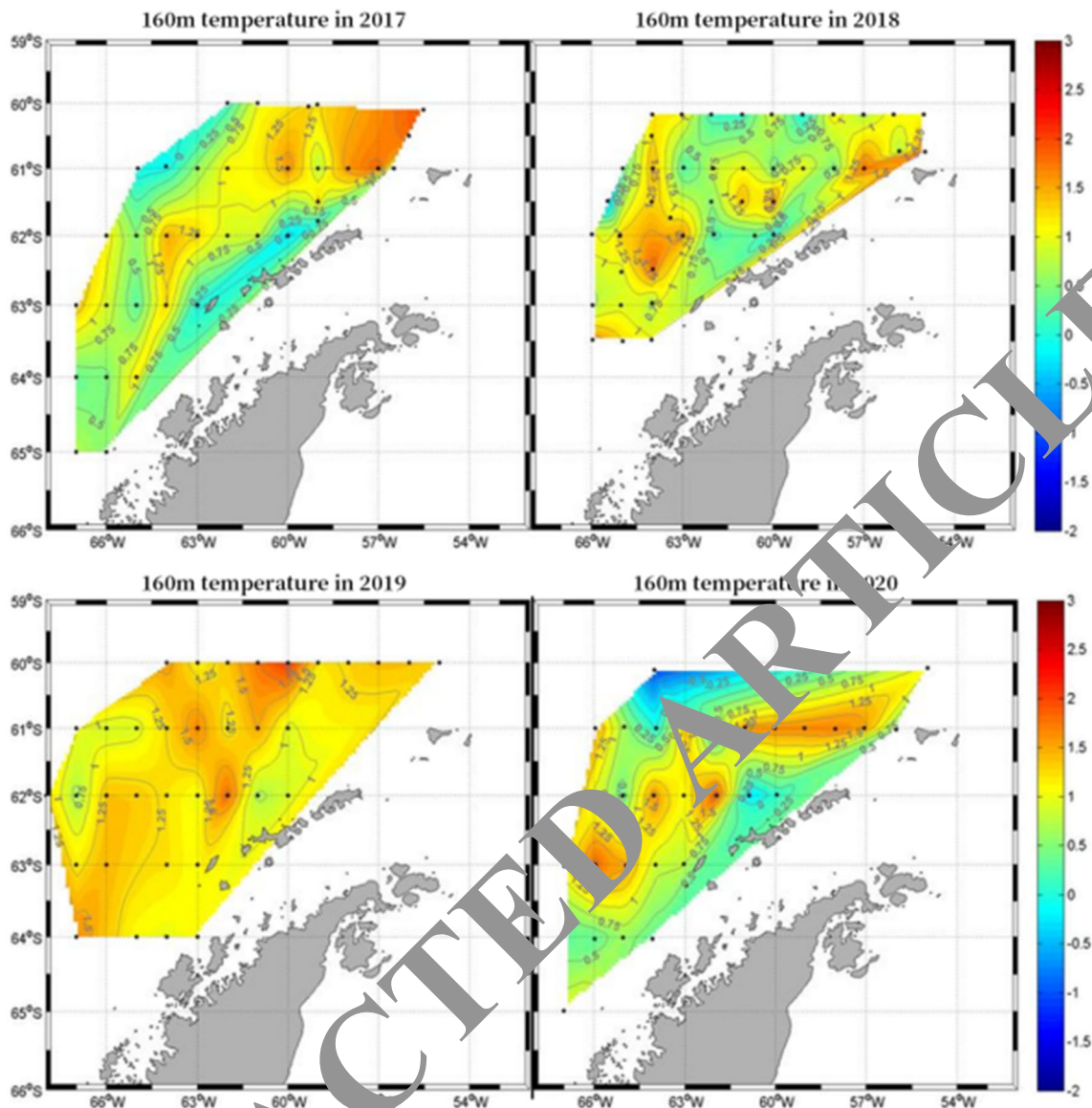


**Fig. 5** Spatial distribution of temperature at 160 meters

In order to better study the spatial distribution of future SST and its changes, we use the highest spatial resolution MPI-ESM-MR simulation results to map the distribution of SST changes in the continental shelf sea of eastern China in 2030, 2060, and 2090 and relative to 2010. As shown in Fig. 9, it is found that in 2030, compared with 2010, the East China Sea, especially the coastal waters of Jiangsu and the southwestern part of Jeju Island, will be warming up significantly; by 2060, the continental shelf sea of eastern China will be warming to varying degrees, among which is the Yangtze River. The warming is most obvious near the mouth of the sea and the southeastern part of the East China Sea; by 2090, the eastern shelf sea of eastern China will have a full-scale warming, of which the central and eastern seas of the East China Sea have the largest warming, while the sea near the mouth of the

Yangtze River has a lower temperature increase or even a cooling. As shown in Fig. 10.

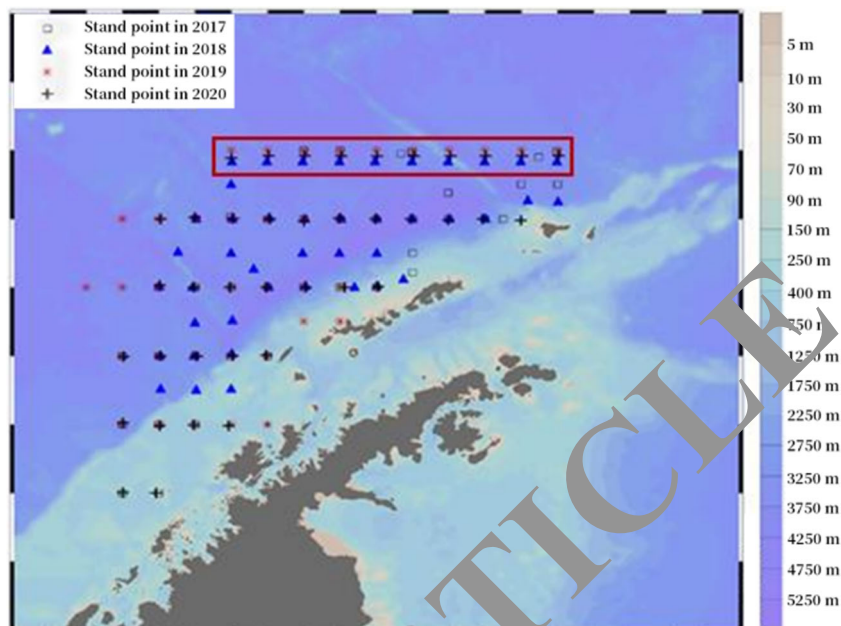
Table 5 shows the SST values of each model in the four seasons of 2030, 2060, and 2090 in the coastal waters of eastern China (Bohai Sea, Yellow Sea, and East China Sea).

Figure 11 shows the predictions of the SST values of the Bohai Sea in the four seasons of 2030, 2060, and 2090 and the changes and rates of change in 2030, 2060, and 2090 relative to the four seasons in 2010.

From Table 6, we find that the future seasonal variation of the Yellow Sea SST will be consistent with the inter-annual variation. In the next 100 years, every season will have an obvious warming trend. From 2010 to 2030, the average temperature of the Yellow Sea will be 0.35–0.51 °C in each season.



**Fig. 6** Station distribution map of section D1



In Fig. 11, the temperature increase in summer is the largest and the minimum in winter; from 2010 to 2060, the average temperature rise in each season is 1.15–1.73°C, with the largest temperature increase in summer and the smallest in winter; from 2010 to 2090, the average temperature rise in each season is 1.46–2.04 °C, the temperature rises the most in summer and the smallest in winter. From the perspective of the inter-annual rate of change, like the Bohai Sea, the Yellow Sea has the largest rate of change in SST from 2030 to 2060 in each season, and the temperature rise slows down from 2060 to 2090, and the change is not obvious.

From Table 7 and Fig. 1, we find that the future seasonal variation of the Yellow Sea SST will be consistent with the inter-annual variation. In the next 100 years, every season will have an obvious warming trend. From 2010 to 2030, the yellow Sea SST will increase by an average of 0.35–0.51 °C, with the largest temperature increase in summer and the smallest in winter; from 2010 to 2060, the average temperature increase in each season is 1.15–1.73 °C, with the largest increase in summer and the smallest in winter; from 2010 to 2090, the average temperature increase in each season is 1.46–2.04°C, with the largest temperature increase in summer and the smallest in winter. From the perspective of the inter-annual rate of change, like the Bohai Sea, the Yellow Sea has the largest rate of change in SST from 2030 to 2060 in each season. The temperature rise will slow down from 2060 to 2090, and the change is not obvious.

Figure 12 shows the SST values of each model for the East China Sea in the four seasons of 2030, 2060, and 2090. We find that the future SST changes in the East China Sea in each season will be consistent with the inter-annual changes, and there will be an obvious warming trend in the next 80 years.

As shown in Fig. 13, from 2010 to 2030, the average temperature rise of SST in the East China Sea in each season is 0.41–0.45°C, of which the temperature rise in summer is the largest and the smallest in winter; from 2010 to 2060, the temperature rises in each season is 0.9–1.11 °C.

## Discussion

### The linguistic and cultural characteristics of trade English

As a practical style, business English not only has unique vocabulary and syntactic functions that make it different from ordinary languages, but also has unique professional knowledge and cultural background.

#### Cultural characteristics

The carrier of culture is language. Each language contains specific cultural information, and business English is no exception. Therefore, the communication process between the company and the retailer also includes the transmission of certain cultural information. As the nations have different historical backgrounds, customs, and cultural traditions, the objective existence of such cultural differences inevitably affects business contacts.

#### Vocabulary features

Business English is more rigorous and formal and often contains technical terms, such as FOB (Free On Board),

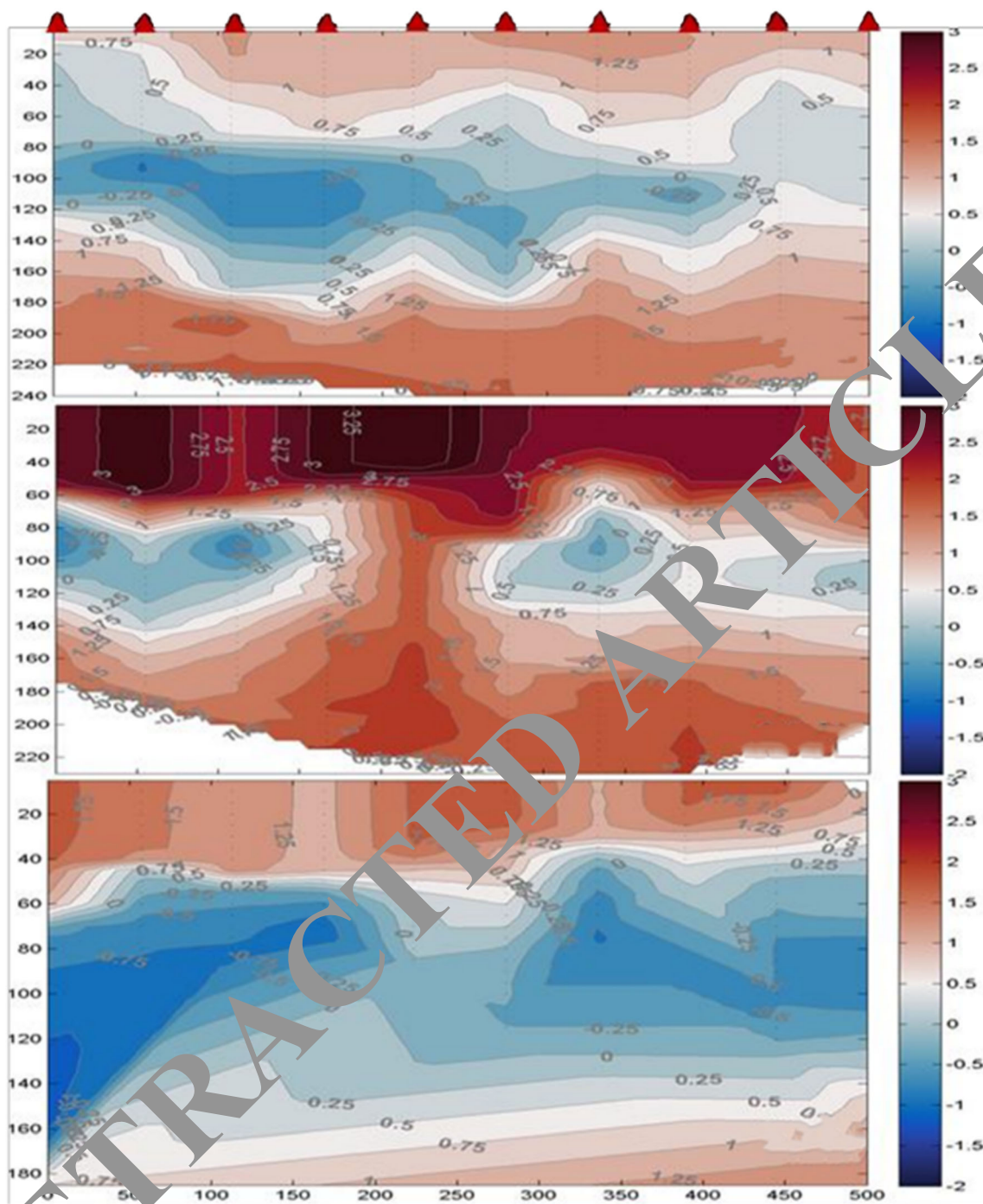


Fig. 7 Temperature and salinity distribution map of section D1 in 2018, 2019, and 2020

**Table 3** Differences between CMIP5 model data and actual observational data WOA13 V2 simulation results of surface water temperature in 2010 (unit: °C)

Data sources		The annual average	Spring	Summer	Autumn	Winter
WOA13 V2		18.08	16.79	25.79	18.54	11.19
CMIP5 model error	ACCESS1.3	- 0.67	- 1.49	- 2.42	0.60	0.62
	BCC-CSM1.1	0.35	- 0.68	- 0.77	1.87	0.92
	CCSM4	0.33	- 0.77	- 0.14	1.49	0.72
	GFDL-ESM2G	0.47	- 0.53	- 0.25	1.53	0.73
	MPI-ESM-MR	0.15	- 0.96	- 0.80	1.65	0.72

**Table 4** Estimates of future SST (°C), SST change (°C), and rate of change (°C/a) in the coastal waters of eastern China (Bohai Sea, Yellow Sea, East China Sea) by each model (divided into decadal and average)

Model	Sea area	2010	2030	2060	2090	2030–2010 annual change	2060–2010 annual change	2060–2030 annual change
ACCESS1.3	Bohai	10.96	11.40	13.77	13.87	0.44	2.41	0.064
	Yellow Sea	12.47	12.94	14.76	15.29	0.47	2.29	0.059
	East China Sea	22.46	23.18	24.08	24.60	0.71	1.61	0.029
BCC-CSM1.1	Bohai	11.05	11.69	12.29	12.74	0.64	1.24	0.033
	Yellow Sea	12.20	12.89	13.48	13.91	0.69	1.28	0.032
	East China Sea	22.15	22.45	23.05	23.04	0.30	0.90	0.020
CCSM4	Bohai	12.72	12.79	14.05	14.00	0.07	1.33	0.041
	Yellow Sea	14.29	14.39	15.71	15.59	0.10	1.12	0.043
	East China Sea	23.65	23.93	24.62	24.70	0.27	0.96	0.022
GFDL-ESM2G	Bohai	12.56	13.09	13.70	13.79	0.53	1.15	0.020
	Yellow Sea	13.55	14.06	14.72	14.77	0.51	1.17	0.021
	East China Sea	22.18	22.60	22.99	22.73	0.41	0.80	0.013
MPI-ESM-MR	Bohai	13.62	13.89	14.49	14.93	0.27	0.87	0.019
	Yellow Sea	14.57	14.84	15.61	16.03	0.26	0.94	0.022
	East China Sea	23.36	23.84	24.21	24.45	0.48	0.85	0.012
Mode average	Bohai	12.78	12.57	13.58	13.89	0.39	1.40	0.033
	Yellow Sea	13.44	13.84	14.85	15.13	0.41	1.42	0.033
	East China Sea	22.76	23.20	23.79	23.94	0.44	1.03	0.019

Counteroffer (Counter-offer), and Zeit-L/C (Preliminary Letter of Credit). Accurate translation requires a certain basis of professional knowledge. In addition, word ambiguity often appears in business English.

### Sentence features

There are many differences between business English and Chinese sentence patterns. The most obvious aspect is reflected in the widespread use of compound sentences and passive voice in business English. Active voice is more common in Chinese, but due to fluency and coherence and other factors, the passive voice is widely used in business English textbooks. The translation follows Chinese usage and is not improperly restricted by the order of words and the structure of the original text. In addition, complex, multi-level compound long sentences are usually expressed in business English. This is especially true

for formal business styles. It rarely uses simple sentences (such as business contracts), but uses a “tree structure” with subordinate clauses and subordinate clauses.

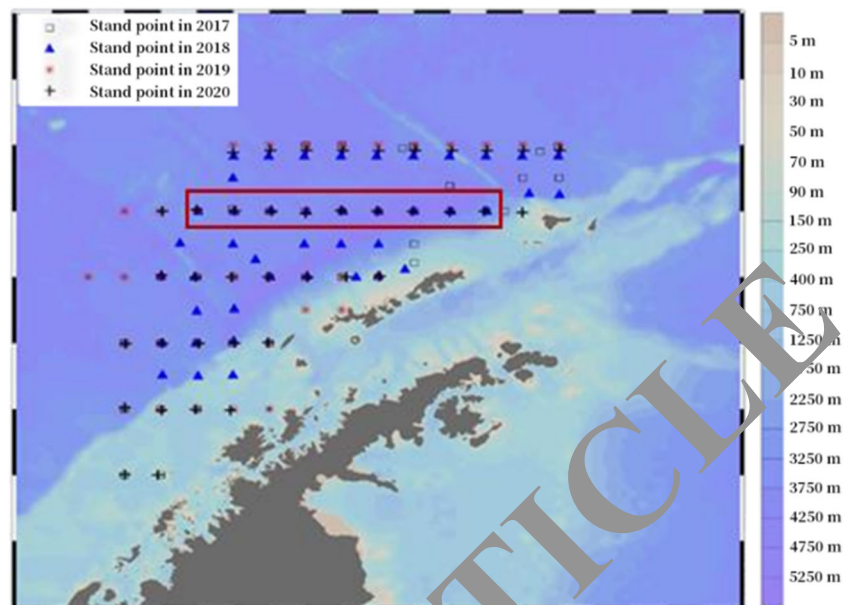
### Errors in the translation of business English vocabulary and their main reasons

In business English vocabulary, translation errors caused by misunderstandings are relatively common in business English translation. Most importantly, errors are caused by fictitious nouns, word ambiguities, and plural nouns.

#### Errors caused by ambiguity

There is ambiguity in English and Chinese, which is very common. Therefore, one of the most important translation problems is to analyze and understand the specific meaning

**Fig. 8** Station distribution map of section D2 (in the red line frame)



of polysemous words in the original language in a given language environment and accurately reproduce them in the target language. Many commonly used English words have common meanings in business English, but they have also acquired new meanings, some of which have evolved into specific vocabulary and foreign trade terms, and have also affected business English and caused many translation errors.

#### Errors caused by virtual nouns

In many cases, abstract nouns in business English can also be countable nouns, which express more specificity and have plural forms. These abstract nouns with virtual and real meanings can be accurately expressed in English. Under these circumstances, the translation must make the nebulous composition a reality, make it more specific, and make the translated article more in line with the original intent. When used as an uncountable noun, imports does not mean “imports” in the abstract, but refers to “imported goods.” The word is used as a countable noun, and its meaning is judged as “delivered goods” to make it more accurate. A little flexibility is needed when dealing with similar situations, and accurate Chinese translation can be achieved by appropriate extensions or additions according to the meaning of the original words.

#### Principles of English vocabulary translation of trade contracts based on functional equivalence translation theory

##### Principles of professionalism

Business English itself is a relatively professional language. English business contracts have legal effect. Whether it is

contract translation in the original language itself, more formal and standardized forms of expression are required, and very strict professional standards are followed. Therefore, when translating foreign trade contracts, it is necessary to adhere to the principle of professional translation, and under the functional equivalence translation theory, its original meaning remains unchanged. For example, the “by virtue of” in a contract is usually translated as “reason,” and “because of” or “due to” are rarely used. Terms such as technical terms and legal terms are often used in English business contracts. These words have been recognized by related disciplines and are basically impossible to cause ambiguity. The meaning of words is fixed and cannot be changed casually. When translating business contracts into English, following professional principles can reduce the complicated interpretation process of the contract, correspondingly reduce the transaction process, and improve the efficiency of transaction activities to a certain extent.

##### Principle of accuracy

The translation of business English contracts must be correct and comply with the principle of accuracy. In addition to complying with the general content of the accuracy principle, the principle also requires its own requirements for the translation of foreign trade contracts. In order to determine contract translation based on the functional equivalence theory, it is necessary to check whether the reader’s response to the translation corresponds to the original viewer’s response to the original text. Therefore, the translator should compare the original contract language with the translation contract language and check whether they are functionally equivalent, that is, whether the foreign businessman’s response to the English

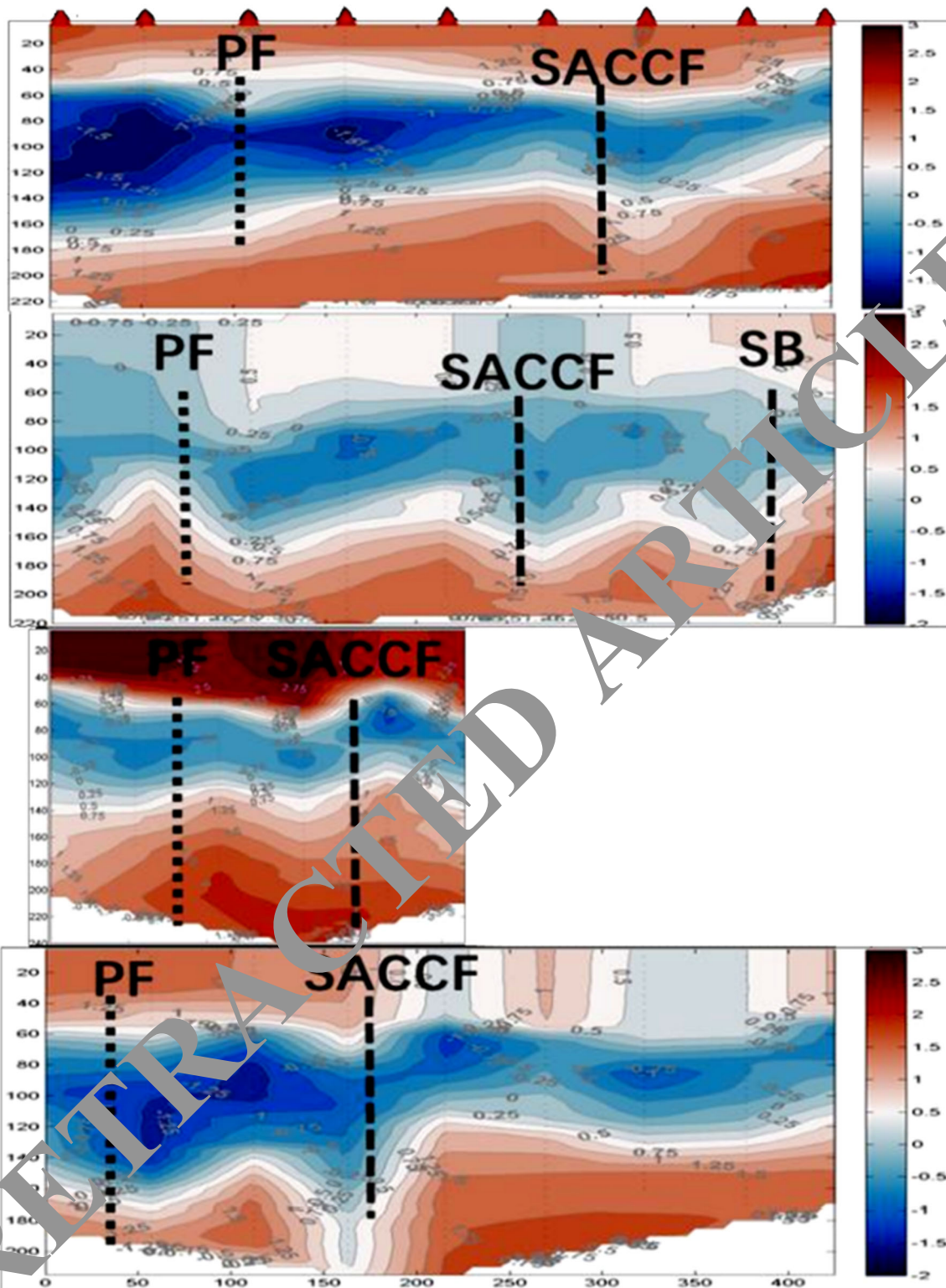


Fig. 9 Inter-decadal projections of the future sea surface temperature (SST) and its changes in the coastal waters of eastern China by each model

translation contract is roughly the same as the Chinese businessman’s response to the Chinese contract and at the same time adheres to the principle of accuracy. Even

small words can be decompiled and are prone to errors. Therefore, it is necessary to realize the correctness of all the terms of the business contract and each word.

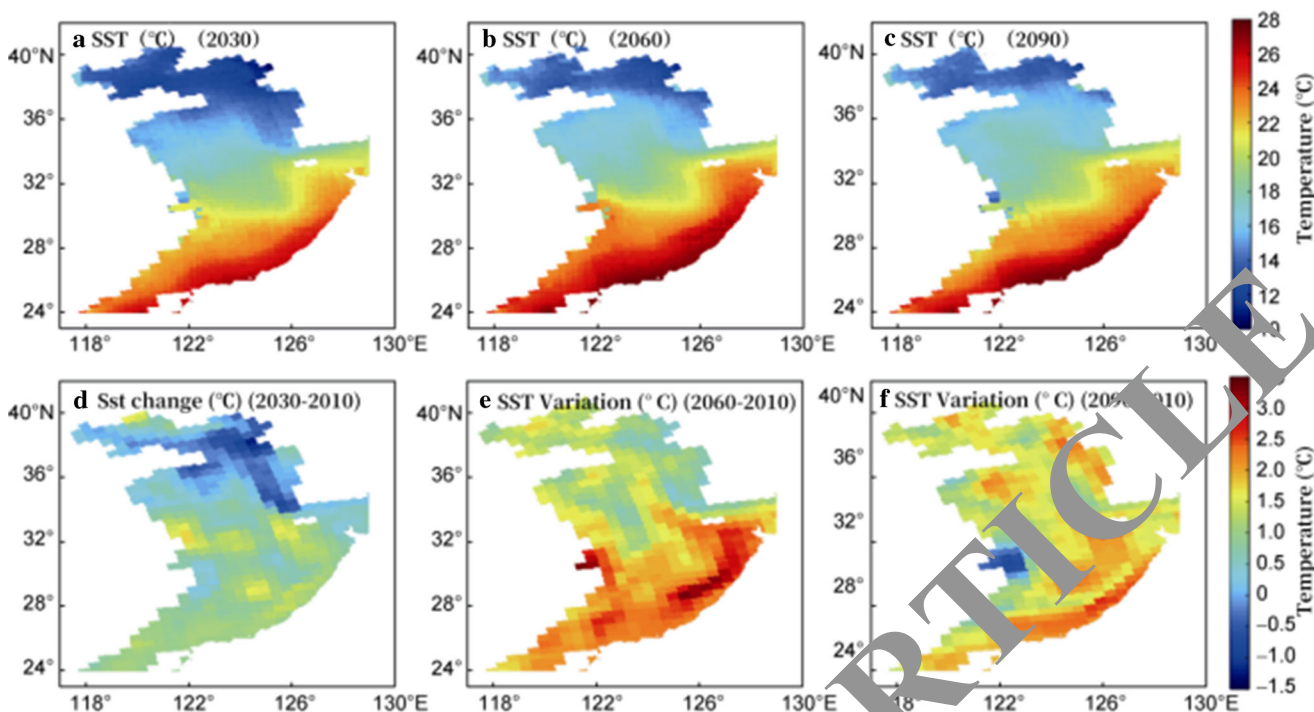


Fig. 10 The change of SST in the coastal waters of eastern China in 2030, 2060, and 2090 estimated using MPI-ESM-MR compared to 2010

**Table 5** Each model’s prediction of the future SST change (°C) and rate of change (°C/a) in the Bohai Sea in spring, summer, autumn, and winter

Model	Season	2030	2060	2090	2030–2010 annual change	2060–2010 annual change	2060–2030 annual rate of change
ACCESS1.3	Spring	7.78	9.70	10.00	0.35	2.28	0.062
	Summer	16.19	16.42	17.00	0.61	2.93	0.075
	Autumn	15.12	17.24	17.90	0.44	2.56	0.068
	Winter	8.59	10.11	10.58	0.34	1.86	0.049
BCC-CS 11.1	Spring	7.08	7.61	7.98	0.58	1.11	0.017
	Summer	19.83	20.67	21.17	0.70	1.54	0.027
	Autumn	15.33	16.15	16.57	0.56	1.38	0.027
	Winter	4.52	4.72	5.24	0.73	0.94	0.007
CCSM4	Spring	6.56	7.84	7.56	0.24	1.52	0.041
	Summer	21.71	22.67	22.82	0.40	1.37	0.031
	Autumn	18.33	19.65	19.75	0.16	1.48	0.043
	Winter	4.56	6.04	5.82	-0.52	0.96	0.048
GFDL-ESM2G	Spring	8.88	9.75	9.54	0.55	1.42	0.028
	Summer	22.31	23.23	23.18	0.67	1.59	0.030
	Autumn	16.15	16.34	16.73	0.32	0.51	0.006
	Winter	5.03	5.49	6.13	0.61	1.07	0.015
MPI-ESM-MR	Spring	9.33	10.06	10.44	0.39	1.13	0.024
	Summer	21.24	22.06	22.74	-0.24	0.58	0.026
	Autumn	18.61	19.00	19.45	0.18	0.58	0.013
	Winter	6.38	6.82	7.11	0.75	1.18	0.014
Mode average	Spring	7.93	8.99	9.11	0.42	1.49	0.034
	Summer	19.84	21.01	21.38	0.43	1.60	0.038
	Autumn	16.70	17.68	18.08	0.33	1.30	0.031
	Winter	5.82	6.63	6.98	0.38	1.20	0.027

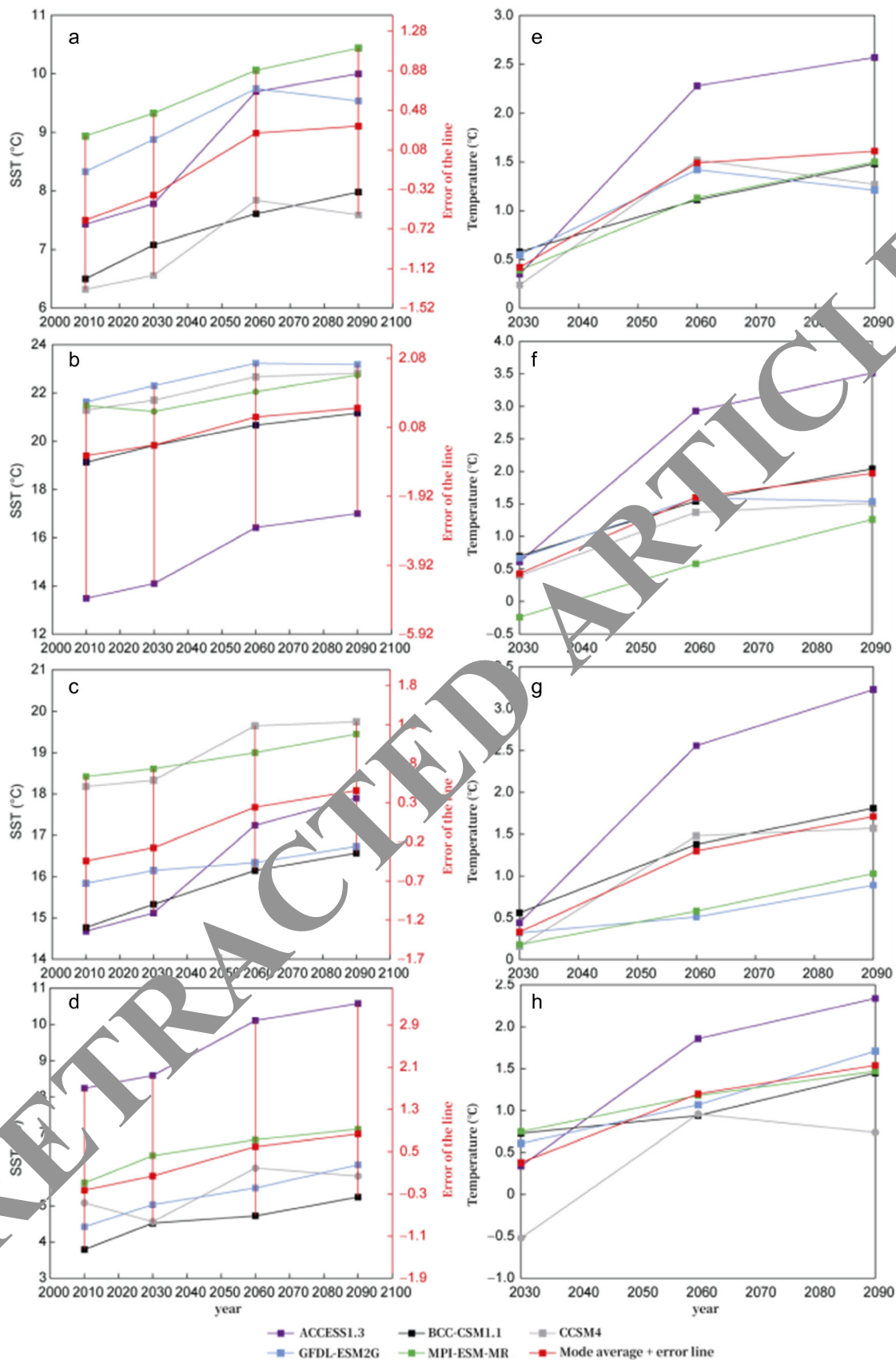


Fig. 11 The prediction of SST and its changes in the future Bohai Sea in spring, summer, autumn, and winter by each model

**Table 6** Each model's estimation of the future SST change (°C) and rate of change (°C/year) of the Yellow Sea in spring, summer, autumn, and winter

Model	Season	2030	2060	2090	2030–2010 annual change
ACCESS1.3	Spring	8.70	10.50	10.79	0.31
	Summer	15.76	17.90	18.50	0.63
	Autumn	17.88	19.90	20.60	0.55
	Winter	9.41	10.74	11.28	0.39
BC-CSM1.1	Spring	7.86	8.26	8.60	0.66
	Summer	17.67	18.53	19.05	0.69
	Autumn	18.15	19.04	19.44	0.61
	Winter	7.87	8.07	8.56	0.77
CCSM4	Spring	8.27	9.60	9.39	0.20
	Summer	22.10	23.25	23.41	0.43
	Autumn	20.16	21.39	21.38	0.18
	Winter	7.02	8.58	8.55	0.42
GFDL-ESM2G	Spring	9.47	10.31	10.17	0.36
	Summer	21.84	22.97	22.62	0.82
	Autumn	17.50	17.82	18.00	0.42
	Winter	7.43	7.80	8.42	0.43
Mode average	Spring	8.85	9.85	10.01	0.39
	Summer	19.83	21.05	21.37	0.51
	Autumn	18.77	19.74	20.04	0.38
	Winter	7.97	8.77	9.09	0.35

**Table 7** Each model's estimation of the future SST change (°C) and rate of change (°C/year) in the East China Sea in spring, summer, autumn, and winter

Model	Season	2030	2060	2090	2030–2010 annual change
ACCESS1.3	Spring	20.69	21.70	22.07	0.65
	Summer	25.65	26.96	27.37	0.56
	Autumn	25.72	26.59	27.11	0.83
	Winter	20.64	21.07	21.84	0.80
BCC-CSM1.1	Spring	19.49	19.95	19.88	0.40
	Summer	25.76	26.63	26.62	0.03
	Autumn	25.40	26.06	25.96	0.41
	Winter	19.15	19.56	19.70	0.35
CCSM4	Spring	21.29	22.00	22.18	0.23
	Summer	28.02	28.45	28.74	0.27
	Autumn	26.68	27.24	27.39	0.50
	Winter	19.72	20.78	20.50	0.09
GFDL-ESM2G	Spring	19.40	19.83	19.68	0.57
	Summer	27.52	28.07	27.67	0.63
	Autumn	24.90	25.33	25.33	0.07
	Winter	18.57	18.71	19.03	0.39
Mode average	Spring	20.33	20.93	21.08	0.44
	Summer	27.01	27.68	27.77	0.45
	Autumn	25.84	26.45	26.56	0.44
	Winter	19.61	20.09	20.36	0.41



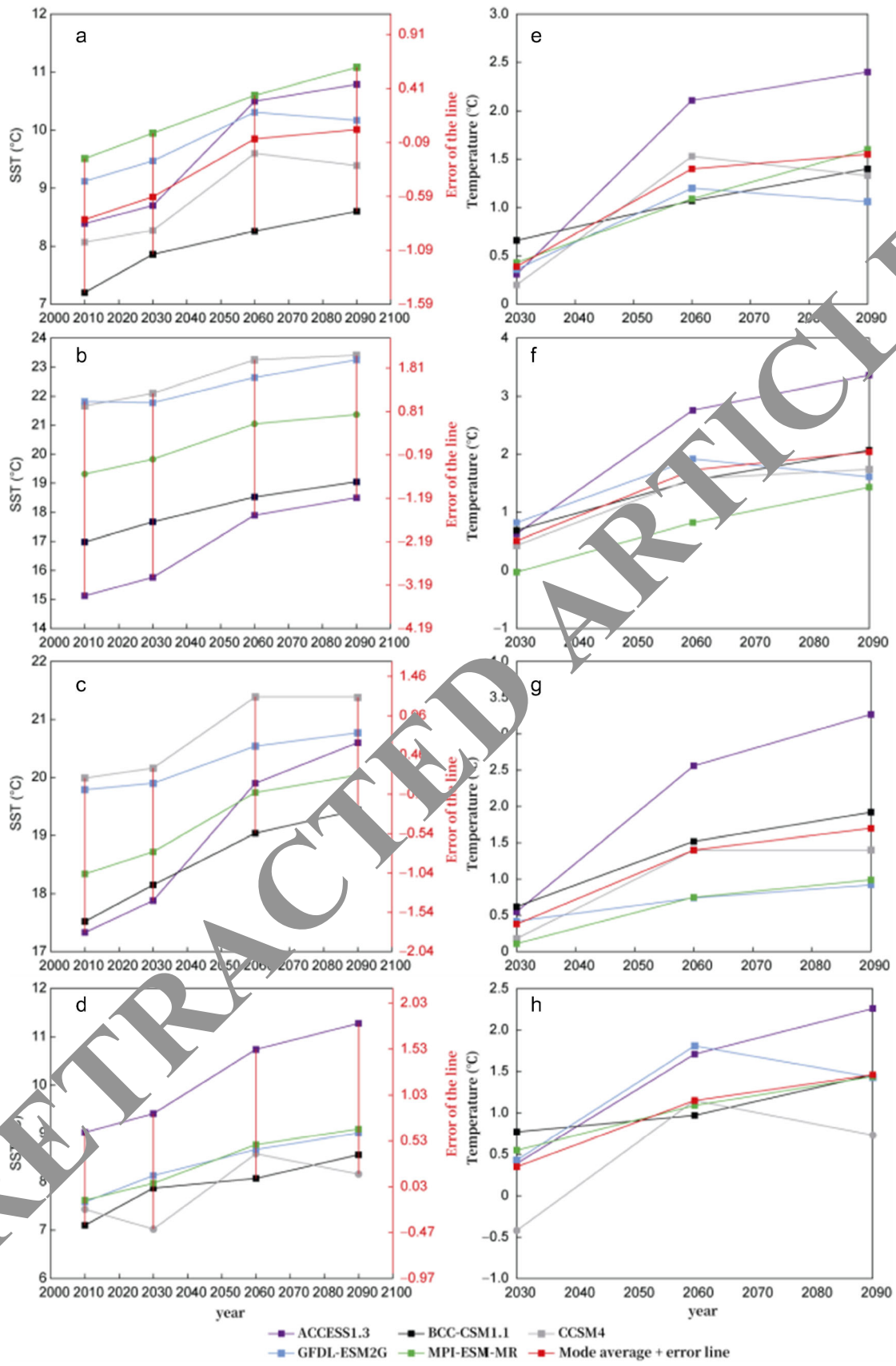


Fig. 12 The forecast of SST and its changes in the future of the Yellow Sea in spring, summer, autumn, and winter by each model

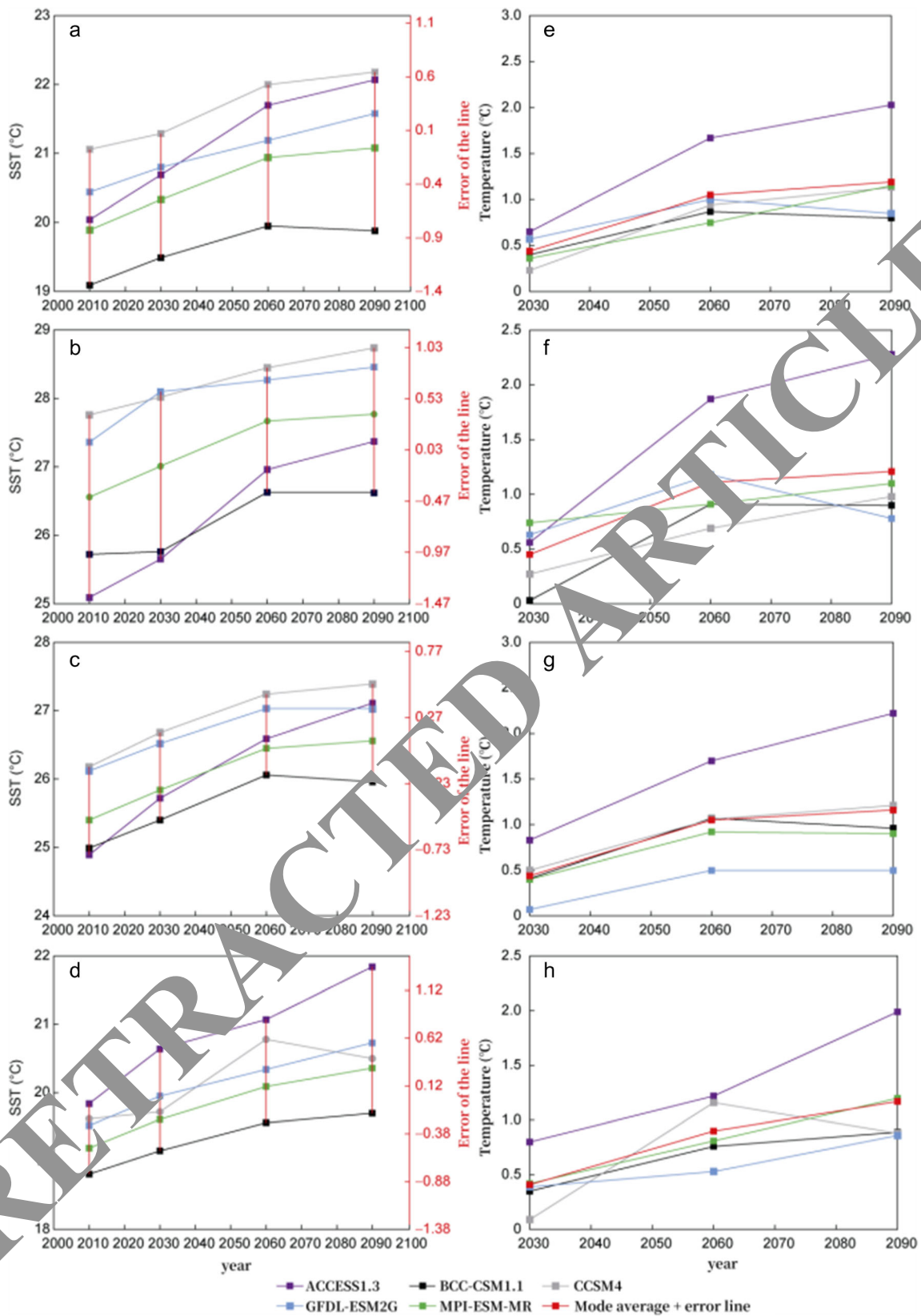


Fig. 13 Each model’s prediction of SST and its changes in the spring, summer, autumn, and winter of the East China Sea in the future

## Application of English vocabulary translation in business contracts based on functional equivalence translation theory

Nida's equivalent function translation theory is mainly that the recipient's response to the translation is essentially the same as the recipient's response to the original text. According to Nida's theory, commenting on the advantages and disadvantages of the translation depends on whether the viewer's reaction to the translation is similar to the reader's reaction to the original text. The word translation serves the viewer and depends on the viewer. The focus is on whether the translation can be understood correctly.

### Lexical equivalence

According to the translation theory of functional equivalence, follow the principle of lexical equivalence while paying attention to the flexibility of translation. When translating business contracts, the translation method is a relatively common translation method, which mainly involves the nature of words in the source language, but they may not always have the same meaning when they are put into the target language. When using the conversion method to translate a business contract, it is necessary to translate a certain language in the English contract into another meaning in Chinese, or translate a certain language in Chinese into another meaning in English. One of the most common is the conversion of English nouns to Chinese verbs. "Delivery" is a noun, but in Chinese translation, delivery is translated as "delivery" belonging to a verb, and the subject is converted into a predicate. In this case, the subject of the original text (if it is a gerund and belongs to the passive voice) can be converted. In the business contract, the conditions related to transportation, packaging, payment, and inspection are basically passive statements. When translating such sentences, they can be translated into active sentences, which is more in line with Chinese writing language style.

### Text equivalent

In the translation of business contracts based on the functional equivalence theory, text equivalence should be achieved, and the translated text should conform to the English stylistic characteristics as much as possible (depending on information equivalence) so that foreign traders can express clear contract information. A business English contract is a legal document that must meet strict requirements and standards, because the main purpose of translating a business English contract is to promote communication between business and culture. The repeated use of vocabulary will emphasize these contractual features, but when translated into Chinese, according to the characteristics of Chinese, it is not necessary to translate complicated synonyms one by one. Words can be used to express

meaning, but words that have no actual meaning in the contract should be deleted. For example, in English business contracts, many adverbial clauses and defined clauses are often mixed with other modifiers to explain or supplement the meaning of the main clause. There is a big difference in expression between English and Chinese. Translators cannot directly translate these sentences into Chinese. Some sentences can be broken down correctly, and the order of words can be adjusted to comply with the textual equivalence principle and better express the meaning of the contract.

### Sentence and meaning equivalence

According to the theory of functional equivalence, the focus of translation is the information content of the translation. According to the principle of information equivalence, it is necessary to effectively translate the information in the business English contract and translate the original information as accurately as possible. When the commercial contract was drafted, it was carefully planned and reviewed by the contractor. Each of these words has a specific meaning. The main task of translating business contracts is to translate between various languages. During the conversion process, the original text must match the target text. Therefore, translators must have a high level of English professionalism and adhere to the principle of consistency between the translation and the original text, which cannot be used subjectively emotionally to avoid unnecessary problems. In order to achieve information equivalence, not only must standards be written, but also spelling and grammatical errors must be avoided, and literal translation and incorrect translation must be avoided as much as possible. Nida's functional equivalence theory suggests that if the content of the original work remains in the translation, the form must be changed. English translation is usually not available for fixed translation, and the translation of business contracts is no exception.

### Conclusion

All in all, business contracts have a special language function, which defines the rights and obligations of both parties to the transaction and is an important basis for reducing disputes. Therefore, in the new era, attention should be paid to the translation of English vocabulary in business contracts, and it is necessary to achieve vocabulary equivalence, sentence meaning equivalence, and text equivalence on the basis of observing functional equivalence theory. In order to promote the development of business activities, it is necessary to translate relatively appropriate business contracts according to the language usage, and the translation should be rigorous, accurate, and reasonable in wording. Business English also contains some common errors, such as the differences between

Chinese and English and the differences in thinking. The translator does not have sufficient knowledge of Chinese and English and knowledge management skills. With the development of economic life, there are many related words and names that have never been seen before.

## Declarations

**Conflict of interest** The authors declare that they have no competing interests.

## References

- Al-Dossary S, Marfurt KJ (2006) 3D volumetric multispectral estimates of reflector curvature and rotation. *Geophysics* 71(5):P41–P51
- Blakely RJ (1995) *Potential theory in gravity and magnetic applications*. Cambridge University Press 441pp
- Blumentritt CH, Marfurt KJ, Sullivan EC (2006) Volume-based curvature computations illuminate fracture orientations — early to mid-Palaeozoic, Central Basin Platform, west Texas. *Geophysics* 71:159–166
- Cevallos C, Kovac P, Lowe S (2013) Application of curvatures to airborne gravity gradient data in oil exploration. *Geophysics* 78(4):G81–G88
- Cooper GRJ, Cowan DR (2009) Terracing potential field data. *Geophys Prospect* 57:1057–1061
- Eales HV (2001) A first introduction to the geology of the Bushveld complex and those aspects of geology that relate to it. Council for Geoscience, Pretoria 84pp
- Gonzalez RC, Woods RE (2008) *Digital image processing, 3rd edn*. Pearson 976pp
- Lee MD, Morris M, Leblanc G, Harris J (2013) Curvature analysis to differentiate magnetic sources for geologic mapping. *Geophys Prospect* 61:572–585
- Li X (2015) Curvature of a geometric surface and curvature of gravity and magnetic anomalies. *Geophysics* 80(1):G1–G26
- Miller HG, Singh V (1994) Potential field tilt – a new concept for location of potential field sources. *J Appl Geophys* 32:213–217
- Mitasova H, Jaroslav H (1993) Interpolation by regularized spline with tension: II. Application to terrain modelling and surface geometry analysis. *Math Geol* 25:657–669
- Phillips JD, Hansen RO, Blakely RJ (2007) The use of curvature in potential-field interpretation. *Explor Geophys* 38:111–119
- Roberts A (2001) Curvature attributes and their applications to 3D interpreted horizons. *First Break* 19(2):85–100
- Sandgren P, Snowball I (2001) Application of mineral magnetic techniques to paleolimnology BT - tracking environmental change using lake sediments: physical and geochemical methods. In: Smol JP (ed) Last WM. Springer Netherlands, Dordrecht, pp 217–237
- Scofield N, Roggenthen WM (1986) Petrologic evolution of glaucophane-rich cumulates from the Wichita Mountains, Oklahoma: effects upon magnetic remanence properties. *Geology* 14:908–911. [https://doi.org/10.1130/0091-7613\(1986\)14<908:PETOCF>2.0.CO;2](https://doi.org/10.1130/0091-7613(1986)14<908:PETOCF>2.0.CO;2)
- Seisuma Z, Kulikova I (2012) Distribution of metal concentrations in sediments of the coastal zone of the Gulf of Riga and an open part of the Baltic Sea. *Oceanology* 52:780–784. <https://doi.org/10.1134/S0001437012060112>
- Sergeev A (2015) The history of geological development of the Curonian Spit in the Holocene and modern hydrodynamic processes in the coastal zone (in Russian). A.P. Karpinsky Russian Geological Research Institute
- Sergeev AY, Zhamoiyeva A, Ryabovsk DV, Buynevich IV, Sivkov VV, Dorokhov DV, Bitinas A, Pupienis D (2017) Genesis, distribution and dynamics of large-scale marl extrusions along the Curonian Spit, southeast Baltic coast. *Boreas* 46:69–82. <https://doi.org/10.1111/bor.12127>
- Šliaupa S, Hoth (2011) Geological evolution and resources of the Baltic Sea area from the Precambrian to the Quaternary. *Balt Sea Basin - B Ser Cent East Eur Dev Stud*:13–51. [https://doi.org/10.1007/978-3-12-17220-5\\_2](https://doi.org/10.1007/978-3-12-17220-5_2)
- Stauskaitė R (1962) Mineralogical composition of sand from the Baltic Sea coastal stretch between Šventoji- Jantarnoe (Palvinkai). *Proc Sci Acad Lith Ser B* 4:83–105
- Stauskaitė R (1966) Lithology and lithodynamic of modern sediments in the coastal zone of south-east the Baltic Sea. Vilnius
- Tanner WF (1990) Origin of barrier islands on sandy coasts. *Trans Gulf Coast Assoc Geol Soc* 40:819–824. <https://doi.org/10.1306/20b232cd-170d-11d7-8645000102c1865d>
- Vetrimurugan E, Shruti VC, Jonathan MP, Roy PD, Kunene NW, Villegas LEC (2017) Metal concentration in the tourist beaches of South Durban: an industrial hub of South Africa. *Mar Pollut Bull* 117:538–546. <https://doi.org/10.1016/j.marpolbul.2017.02.036>